

# Single-Input Two-Output Boost Converter

Kamarunnisa M M<sup>1</sup>, Ansia Aziz<sup>2</sup>

ICET Mulavoor<sup>1</sup>

Asst Professor, ICET Mulavoor<sup>2</sup>

**Abstract:** The aim of this study is to develop a high-efficiency single-input multiple-output (SIMO) dc–dc converter. The proposed converter can boost the voltage of a low-voltage input power source to a controllable high-voltage dc bus and middle-voltage output terminals. The high-voltage dc bus can take as the main power for a high-voltage dc load or the front terminal of a dc–ac inverter. Moreover, middle-voltage output terminals can supply powers for individual middle-voltage dc loads or for charging auxiliary power sources (e.g., battery modules). In this study, a coupled-inductor-based dc–dc converter scheme utilizes only one power switch with the properties of voltage clamping and soft switching, and the corresponding device specifications are adequately designed. As a result, the objectives of high-efficiency power conversion, high step-up ratio, and various output voltages with different levels can be obtained. Some experimental results via a kilowatt-level prototype are given to verify the effectiveness of the proposed SIMO dc–dc converter in practical applications.

**Index Terms:** Coupled inductor, high-efficiency power conversion, single-input multiple-output (SIMO) converter, soft switching, voltage clamping.

## I. INTRODUCTION

IN ORDER to protect the natural environment on the earth, the development of clean energy without pollution has the major representative role in the last decade [1]–[3]. By dealing with the issue of global warming, clean energies, such as fuel cell (FC), photovoltaic, and wind energy, etc., have been rapidly promoted. Due to the electric characteristics of clean energy, the generated power is critically affected by the climate or has slow transient responses, and the output voltage is easily influenced by load variations [4]–[6]. Besides, other auxiliary components, e.g., storage elements, control boards, etc., are usually required to ensure the proper operation of clean energy. For example, an FC-generation system is one of the most efficient and effective solutions to the environmental pollution problem [7]. In addition to the FC stack itself, some other auxiliary components, such as the balance of plant (BOP) including an electronic control board, an air compressor, and a cooling fan, are required for the normal work of an FC generation system [8], [9]. In other words, the generated power of the FC stack also should satisfy the power demand for the BOP.

Thus, various voltage levels should be required in the power converter of an FC generation system. In general, various single-input single-output dc–dc converters with different voltage gains are combined to satisfy the requirement of various voltage levels, so that its system control is more complicated and the corresponding cost is more expensive. The motivation of this study is to design a single-input multiple-output (SIMO) converter for increasing the conversion efficiency and voltage gain, reducing the control complexity, and saving the manufacturing cost. Patra et al. [10] presented a SIMO dc–dc converter capable of generating buck, boost, and

inverted outputs simultaneously. However, over three switches for one output were required. This scheme is only suitable for the low output voltage and power application, and its power conversion is degenerated due to the operation of hard switching. Nami et al. [11] proposed a new dc–dc multi-output boost converter, which can share its total output between different series of output voltages for low- and high-power applications. Unfortunately, over two switches for one output were required, and its control scheme was complicated. Besides, the corresponding output power cannot supply for individual loads independently. Chen et al. [12] investigated a multiple-output dc–dc converter with shared zero-current-switching (ZCS) lagging leg. Although this converter with the soft-switching property can reduce the switching losses, this combination scheme with three full-bridge converters is more complicated, so that the objective of high-efficiency power conversion is difficult to achieve, and its cost is inevitably increased.

This study presents a newly designed SIMO converter with a coupled inductor. The proposed converter uses one power switch to achieve the objectives of high-efficiency power conversion, high step-up ratio, and different output voltage levels. In the proposed SIMO converter, the techniques of soft switching and voltage clamping are adopted to reduce the switching and conduction losses via the utilization of a low-voltage-rated power switch with a small  $R_{DS(on)}$ . Because the slew rate of the current change in the coupled inductor can be restricted by the leakage inductor, the current transition time enables the power switch to turn ON with the ZCS property easily, and the effect of the leakage inductor can alleviate the losses caused by the reverse-recovery current.

Additionally, the problems of the stray inductance energy and reverse-recovery currents within diodes in the conventional boost converter also can be solved, so that the high-efficiency power conversion can be achieved. The voltages of middle-voltage output terminals can be appropriately adjusted by the design of auxiliary inductors; the output voltage of the high-voltage dc bus can be stably controlled by a simple proportional-integral (PI) control.

This study is mainly organized into five sections. Following the introduction, the converter design and analyses are given in Section II. In Section III, the design considerations of the proposed SIMO converter are discussed in detail. Section IV provides rich experimental results to validate the effectiveness of the proposed converter in practical applications. Finally, some conclusions are drawn in Section V.

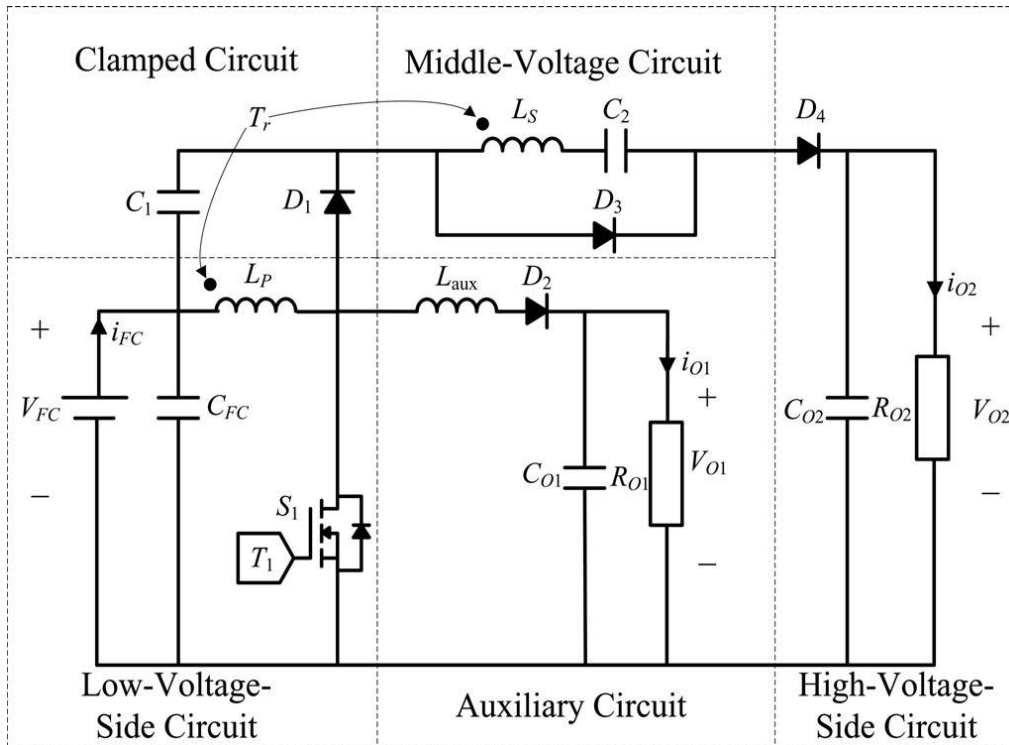


Fig. 1. System configuration of high-efficiency single-input multiple-output (SIMO) converter

## II. CONVERTER DESIGN AND ANALYSES

The system configuration of the proposed high-efficiency SIMO converter topology to generate two different voltage levels from a single-input power source is depicted in Fig. 1. This SIMO converter contains five parts including a low-voltage-side circuit (LVSC), a clamped circuit, a middle-voltage circuit, an auxiliary circuit, and a high-voltage-side circuit (HVSC). The major symbol representations are summarized as follows.  $V_{FC}$  ( $i_{FC}$ ) and  $V_{O1}$  ( $i_{O1}$ ) denote the voltages (currents) of the input power source and the output load at the LVSC and the auxiliary circuit, respectively;  $V_{O2}$  and  $i_{O2}$  are the output voltage and current in the HVSC.  $C_{FC}$ ,  $C_{O1}$ , and  $C_{O2}$  are the filter capacitors at the LVSC, the auxiliary circuit, and the HVSC, respectively;  $C_1$  and  $C_2$  are the clamped and middle-voltage capacitors in the clamped and middle-voltage circuits, respectively.  $L_P$  and  $L_S$  represent individual inductors in the primary and secondary sides of the coupled inductor  $T_r$ , respectively, where the primary side is connected to the input power

source;  $L_{aux}$  is the auxiliary circuit inductor. The main switch is expressed as  $S_1$  in the LVSC; the equivalent load in the auxiliary circuit is represented as  $R_{O1}$ , and the output load is represented as  $R_{O2}$  in the HVSC.

The corresponding equivalent circuit given in Fig. 2 is used to define the voltage polarities and current directions. The coupled inductor in Fig. 1 can be modeled as an ideal transformer including the magnetizing inductor  $L_{mp}$  and the leakage inductor  $L_{kp}$  in Fig. 2. The turns ratio  $N$  and coupling coefficient  $k$  of this ideal transformer are defined as

$$N = N_2 / N_1 \quad k = \frac{L_{mp}}{(L_{kp} + L_{mp})}$$

$$= L_{mp} / L_P \quad (1)$$

$$(2)$$

where  $N_1$  and  $N_2$  are the winding turns in the primary and

sec- ondary sides of the coupled inductor  $T_r$ . Because the voltage gain is less sensitive to the coupling coefficient and the clamped capacitor  $C_1$  is appropriately selected to completely absorb the leakage inductor energy [13], the coupling coefficient could be simply set at one ( $k = 1$ ) to

obtain  $L_{mp} = L_P$  via (2). In this study, the following assumptions are made to simplify the con- verter analyses: 1) The main switch including its body diode is assumed to be an ideal switching element; and 2) The con- duction voltage drops of the switch and diodes are neglected.

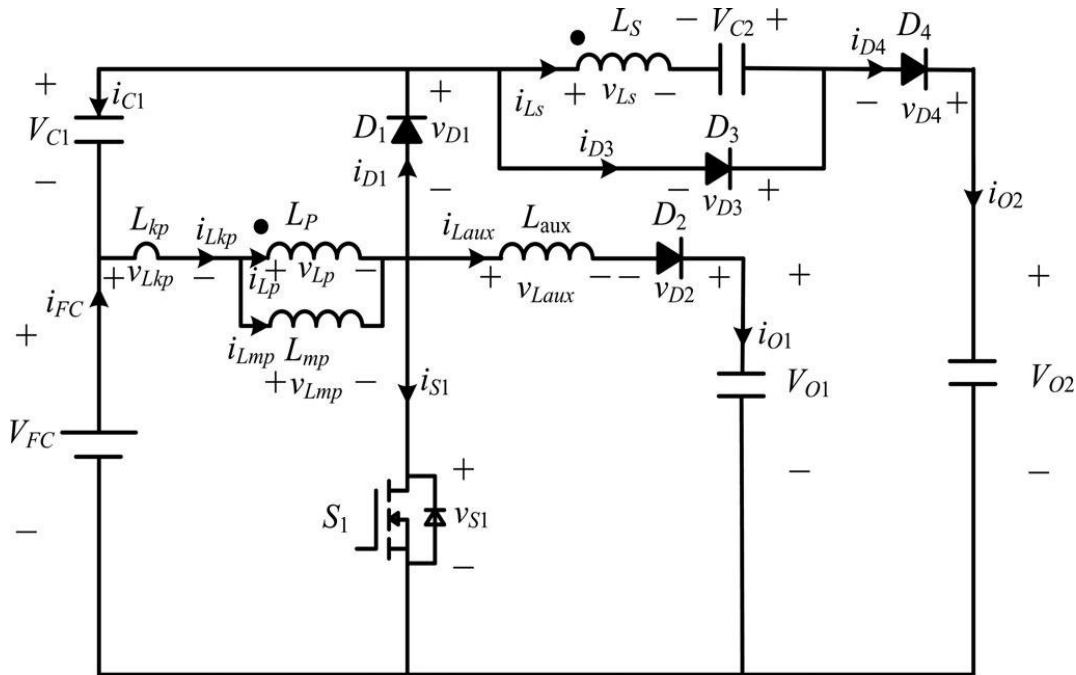


Fig. 2 Equivalent circuit

A. Operation Modes

The characteristic waveforms are depicted in Fig. 3, and the topological modes in one switching cycle are illustrated in Fig. 4.

1) Mode1 ( $t_0-t_1$ )[Fig.4(a)]:In this mode, the main switch  $S_1$  was turned ON for a span, and the diode  $D_4$  turned OFF. Because the polarity of the windings of the coupled inductor  $T_r$  is positive, the diode  $D_3$  turns ON. The secondary current  $i_{L_s}$  reverses and charges to the middle-voltage capacitor  $C_2$ . When the auxiliary inductor  $L_{aux}$  releases its stored energy completely, and the diode  $D_2$  turns OFF, this mode ends.

2) Mode2( $t_1-t_2$ ) [Fig.4(b)]: Attimet= $t_1$ , the main switch  $S_1$  is persistently turned ON. Because the primary inductor  $L_P$  is charged by the input power source, the magnetizing current  $i_{L_{mp}}$  increases gradually in an approximately linear way. At the same time, the secondary voltage  $v_{L_s}$  charges the middle-voltage capacitor  $C_2$  through the diode  $D_3$ . Although the voltage  $v_{L_{mp}}$  is equal to the input voltage  $V_{FC}$  both at modes 1 and 2, the ascendant slope of the leakage current of the coupled inductor ( $di_{L_{kp}}/dt$ ) at modes 1 and 2 is different due to the path of the auxiliary circuit. Because the auxiliary inductor  $L_{aux}$  releases its stored energy completely, and the diode  $D_2$  turns OFF at

the end of mode 1, it results in the reduction of  $di_{L_{kp}}/dt$  at mode 2.

Mode 3 ( $t_2-t_3$ ) [Fig. 4(c)]: At time  $t = t_2$ , the main switch  $S_1$  is turned OFF. When the leakage energy still released from the secondary side of the coupled inductor, the diode  $D_3$  persistently conducts and releases the leakage energy to the middle-voltage capacitor  $C_2$ . When the voltage across the main switch  $v_{S_1}$  is higher than the voltage across the clamped capacitor  $V_{C_1}$ , the diode  $D_1$  conducts to transmit the energy of the primary-side leakage inductor  $L_{kp}$  into the clamped capacitor  $C_1$ . At the same time, partial energy of the primary-side leakage inductor  $L_{kp}$  is transmitted to the auxiliary inductor  $L_{aux}$ , and the diode  $D_2$  conducts. Thus, the current  $i_{L_{aux}}$  passes through the diode  $D_2$  to supply the power for the output load in the auxiliary circuit. When the secondary side of the coupled inductor releases its leakage energy completely, and the diode  $D_3$  turns OFF, this mode ends.

4) Mode4 ( $t_3-t_4$ )[Fig.4(d)]:Attimet= $t_3$ ,themainswitch  $S_1$  is persistently turned OFF. When the leakage energy has released from the primary side of the coupled inductor, the secondary current  $i_{L_s}$  is induced in reverse from the energy of the magnetizing inductor  $L_{mp}$  through the ideal transformer, and flows through the diode  $D_4$  to the HVSC. At the same time, partial energy of the primary- side

leakage inductor  $L_{kp}$  is still persistently transmitted to the auxiliary inductor  $L_{aux}$ , and the diode  $D_2$  keeps conducting. Moreover, the current  $i_{L_{aux}}$  passes through the diode  $D_2$  to supply the power for the output load in the auxiliary circuit.

5) Mode5 ( $t_4-t_5$ )[Fig.4(e)]: Attimet= $t_4$ , the main switch  $S_1$  is persistently turned OFF, and the clamped diode  $D_1$

turns OFF because the primary leakage current  $i_{L_{kp}}$  equals to the auxiliary inductor current  $i_{L_{aux}}$ . In this mode, the input power source, the primary winding of the coupled inductor  $T_r$ , and the auxiliary inductor  $L_{aux}$  connect in series to supply the power for the output load in the aux-iliary circuit through the diode  $D_2$ .

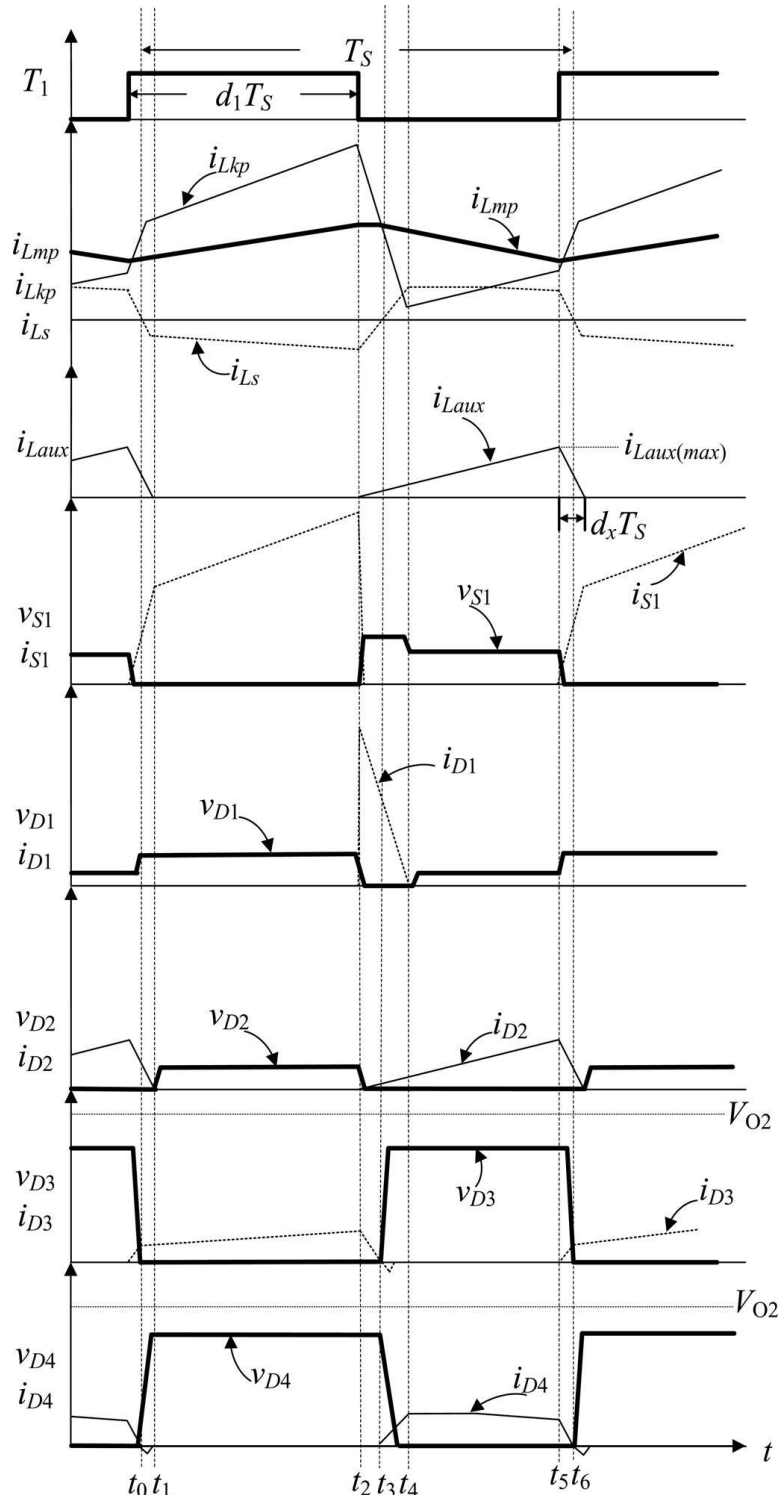


Fig. 3 Characteristic waveforms of high-efficiency SIMO converter

At the same time, the input power source, the secondary winding of the coupled inductor  $T_r$ , the clamped capacitor  $C_1$ , and the middle-voltage capacitor ( $C_2$ ) connect in series to release the energy into the HVSC through the diode  $D_4$ .

6) Mode6 ( $t_5-t_6$ ) [Fig.4(f)]: At  $t=t_5$ , this mode begins when the main switch  $S_1$  is triggered. The auxiliary inductor current  $i_{L_{aux}}$  needs time to decay to zero, the diode  $D_2$  persistently conducts. In this mode, the input power source, the clamped capacitor  $C_1$ , the secondary winding of the coupled inductor  $T_r$ , and the middle-voltage capacitor  $C_2$  still connect in series to release the energy into the HVSC through the diode  $D_4$ . Since the clamped diode  $D_1$  can be selected as a low-voltage Schottky diode, it will be cut off promptly without a reverse-recovery current. Moreover, the rising rate of the primary current  $i_{L_{kp}}$  is limited by the primary-side leakage inductor  $L_{kp}$ .

Thus, one cannot derive any currents from the paths of the HVSC, the middle-voltage circuit, the auxiliary circuit, and the clamped circuit. As a result, the main switch  $S_1$  is turned ON under the condition of ZCS and this soft-switching property is helpful for alleviating the switching loss. When the secondary current  $i_{L_S}$  decays to zero, this mode ends. After that, it begins the next switching cycle and repeats the operation in mode 1.

Remark 1: In general, a dc-dc converter operated at the continuous conduction mode (CCM) can provide a low ripple current for protecting the energy source. In the proposed SIMO converter, it is operated at the CCM due to the design of the auxiliary inductor. The coupled inductor is charged by the input power source when the main switch is turned ON, and the coupled inductor releases its energy to the auxiliary inductor when the main switch is turned OFF until the energy balance of the coupled inductor and the auxiliary inductor is established.

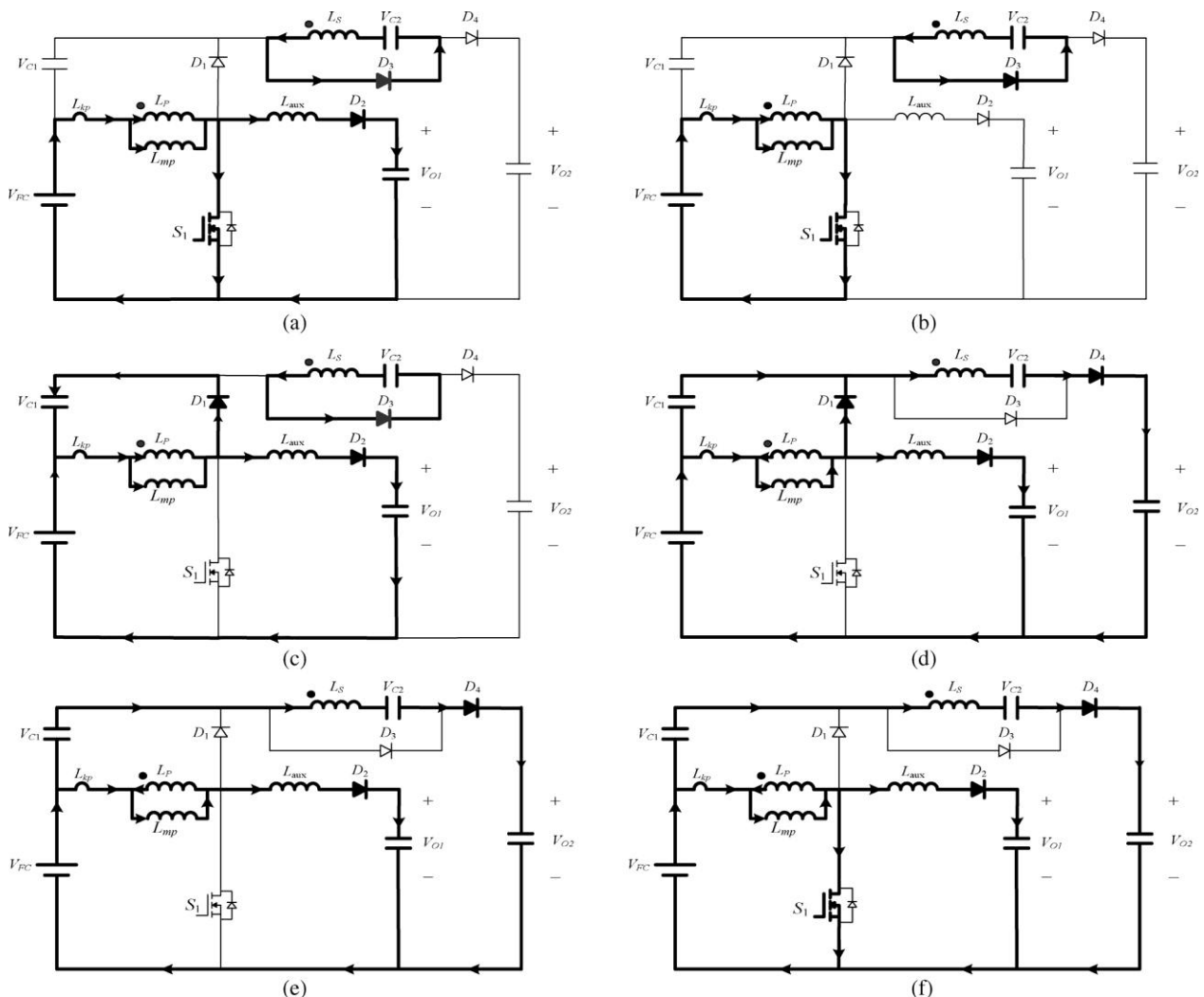
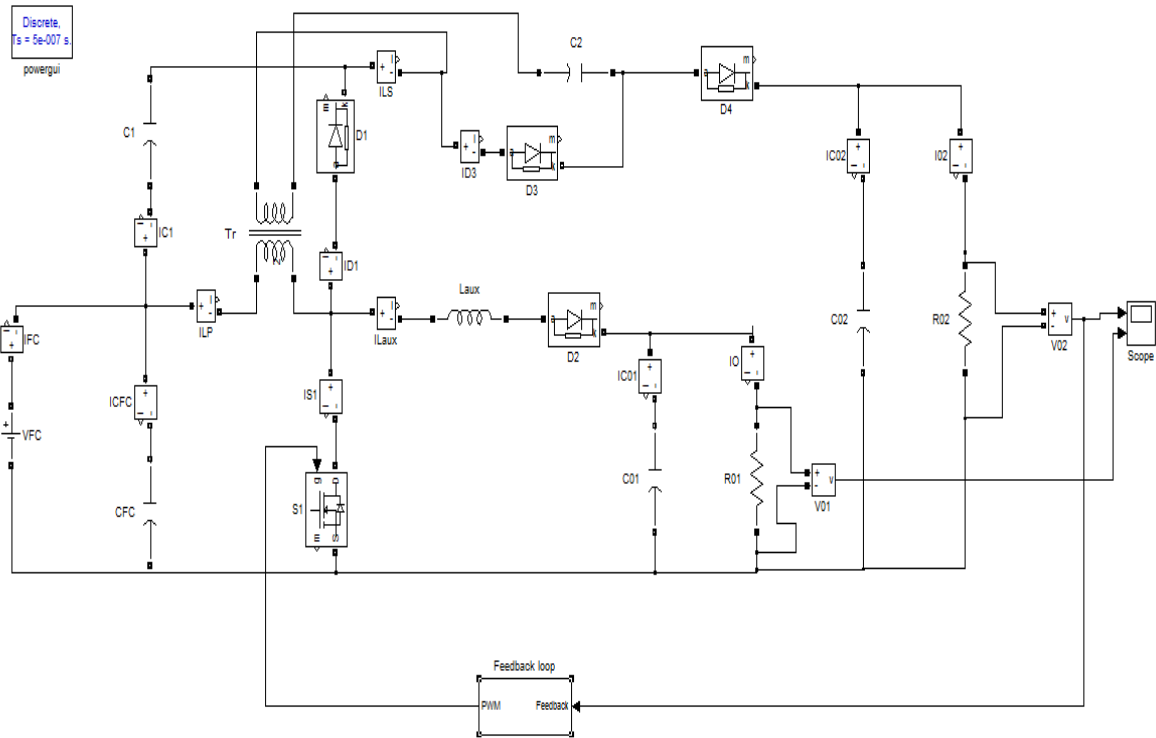


Fig. 4. Topological modes: (a) Mode 1 [ $t_0-t_1$ ]; (b) Mode 2 [ $t_1-t_2$ ]; (c) Mode 3 [ $t_2-t_3$ ]; (d) Mode 4 [ $t_3-t_4$ ]; (e) Mode 5 [ $t_4-t_5$ ]; (f) Mode 6 [ $t_5-t_6$ ].

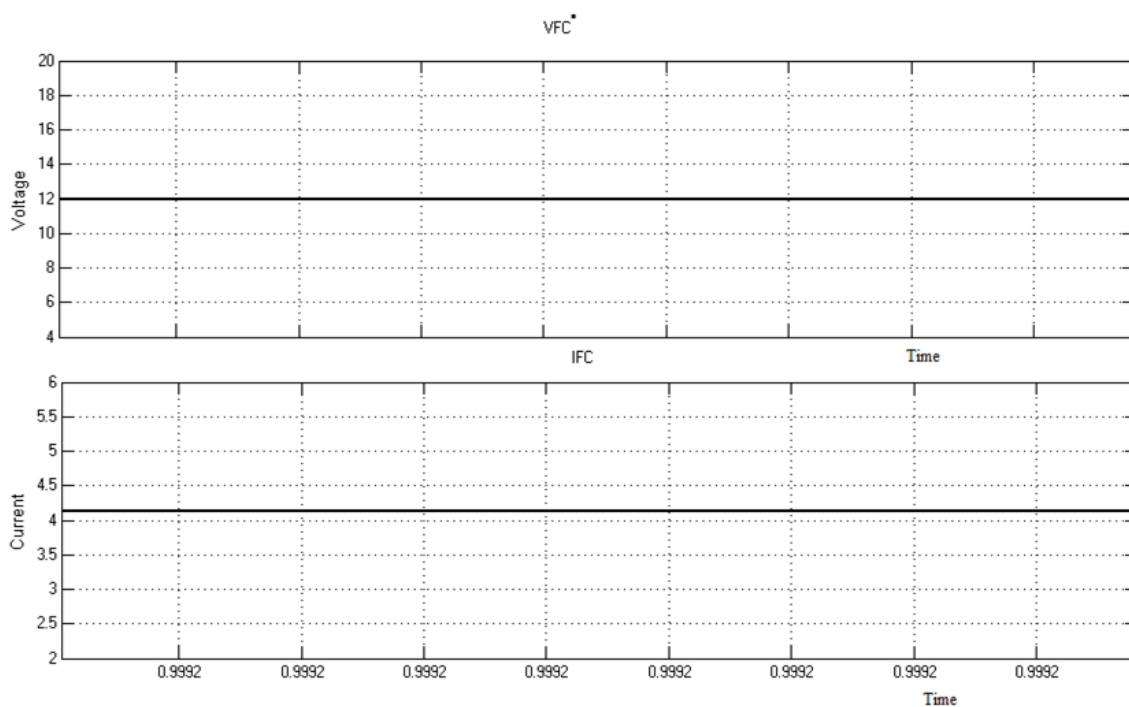
As can be seen from Fig. 3, the primary current of the coupled inductor is positive during one switching cycle. This CCM operation is helpful to extend the lifetime of the input energy source.

### SIMULATION DIAGRAM

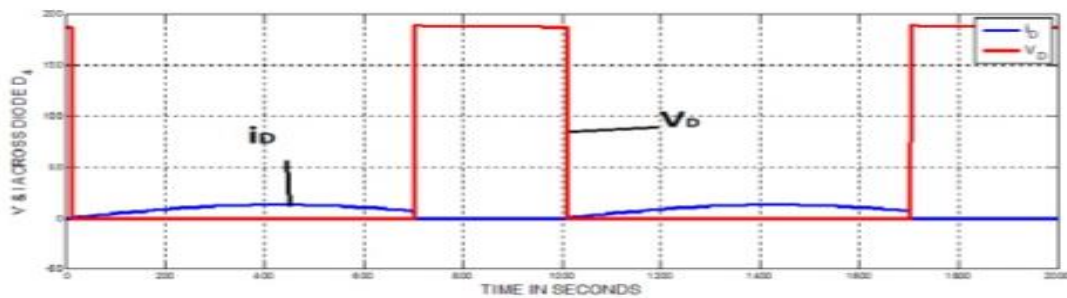
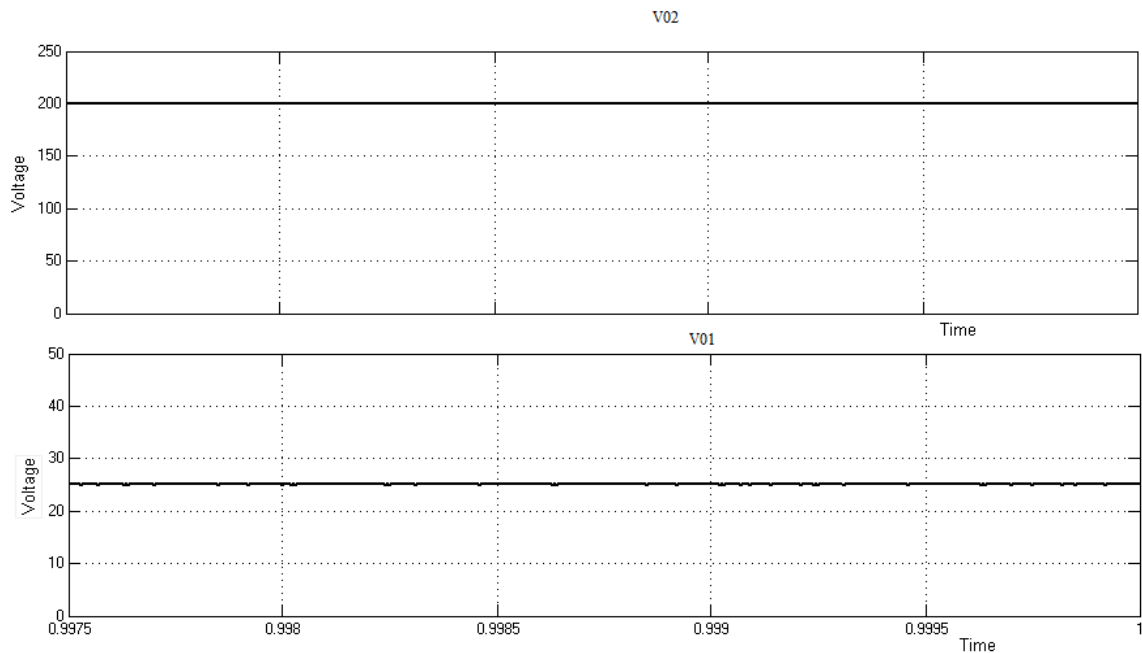


### SIMULATION OUTPUT

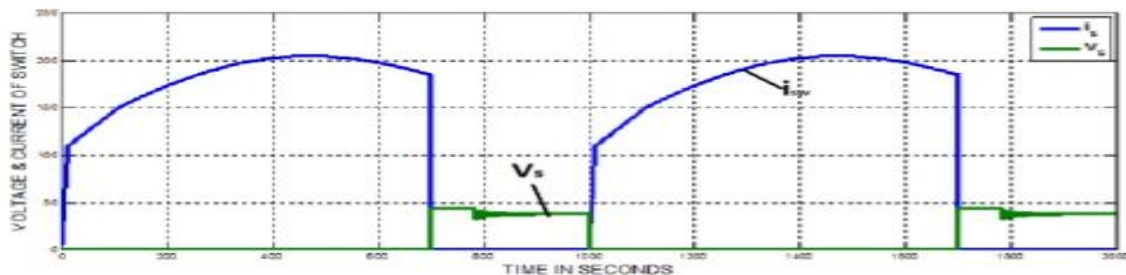
Input voltage and Output current.



## Two Output Voltages



7.3 Voltage & current waveforms across switch



### III. CONCLUSION

This study has successfully developed a high-efficiency SIMO dc–dc converter, and this coupled-inductor-based converter was applied well to a single-input power source plus two output terminals composed of an auxiliary battery module and a high-voltage dc bus. The experimental results reveal that the maximum efficiency was measured to exceed 95%, and the average conversion efficiency was measured over 91%. The proposed SIMO converter is suitable for the application required one common ground, which is preferred in most applications.

However, it is not appropriate to be used as the active front for dc–ac multilevel inverters. This limitation is worthy to be investigated in the future research.

The major scientific contributions of the proposed SIMO converter are recited as follows: 1) this topology adopts only one power switch to achieve the objective of high-efficiency SIMO power conversion; 2) the voltage gain can be substantially increased by using a coupled inductor; 3) the stray energy can be recycled by a clamped



capacitor into the auxiliary battery module or high-voltage dc bus to ensure the property of voltage clamping; 4) an auxiliary inductor is designed for providing the charge power to the auxiliary battery module and assisting the switch turned ON under the condition of ZCS; 5) the switch voltage stress is not related to the input voltage so that it is more suitable for a dc power conversion mechanism with different input voltage levels; and 6) the copper loss in the magnetic core can be greatly reduced as a full copper film with lower turns. This high-efficiency SIMO converter topology provides designers with an alternative choice for boosting a low-voltage power source to multiple outputs with different voltage levels efficiently. The auxiliary battery module used in this study also can be extended easily to other dc loads, even for different voltage demands, via the manipulation of circuit components design.